

Microfabrication of an analog of the basal lamina: biocompatible membranes with complex topographies

GEORGE D. PINS, MEHMET TONER, AND JEFFREY R. MORGAN¹

Center for Engineering in Medicine and Surgical Services, Massachusetts General Hospital, Harvard Medical School and Shriners Burns Hospital, Boston, Massachusetts 02114, USA

ABSTRACT A microfabrication approach was used to produce novel analogs of the basal lamina with complex topographic features. A test pattern of ridges and channels with length scales (40 to 310 μm) similar to the invaginations found in a native basal lamina was laser machined into the surface of a polyimide master chip. Negative replicates of the chip were produced using polydimethylsiloxane silicone elastomer and these replicates were used as templates for the production of thin ($\sim 21 \mu\text{m}$) membranes of collagen or gelatin. The resulting membranes had a complex topography of ridges and channels that recapitulated the features of the master chip. To demonstrate their utility, these complex membranes were laminated to type I collagen sponges and their surfaces were seeded with cultured human epidermal keratinocytes to form a skin equivalent. The keratinocytes formed a differentiated and stratified epidermis that conformed to the features of the microfabricated membrane. The topography of the membrane influenced the differentiation of the keratinocytes because stratification was enhanced in the deeper channels. Membrane topography also controlled the gross surface features of the skin equivalent; infolds of the epidermis increased as channel depth increased. These novel microfabricated analogs of the basal lamina will help to elucidate the influence of topography on epithelial cell proliferation and differentiation and should have applications in the tissue engineering of skin equivalents as well as other basal lamina-containing tissues.—Pins, G. D., Toner, M., Morgan, J. R. Microfabrication of an analog of the basal lamina: biocompatible membranes with complex topographies. *FASEB J.* 14, 593–602 (2000)

Key Words: tissue engineering · basal lamina · dermal analog · polyimide chip

TISSUE ENGINEERING IS an emerging field that seeks to produce replacements for a variety of human tissues and organs in need of repair or restoration (1). These engineered tissue analogs, often com-

posed of cultured cells, biomaterials or composites combining cells and biomaterials, have achieved some clinical success as substitutes for skin and cartilage (2–5). Future developments in the design of tissue substitutes will be aided by an improved understanding of the role of 3-dimensional scaffolds in the regulation of cell function, maintenance of tissue architecture, and the regeneration of important tissue features. Significant effort has been devoted to producing biocompatible scaffolds with defined pore sizes that help ensure proper cell–cell contacts, cell–matrix interactions, and preserve cellular function. For example, in collagen sponges the average pore diameter (skin: 20 to 125 μm , nerve: 5 to 10 μm) and orientation (skin: random, nerve: axial) are critical for optimal analog activity (6, 7). The pore size ($\approx 500 \mu\text{m}$) of cylindrical poly(L-lactic acid) (PLLA) devices also enhances the rate of fibrovascular tissue growth into porous 3-dimensional scaffolds (8). Likewise, 12 μm diameter polyglycolic acid (PGA) fibers processed into 96–97% porous, nonwoven meshes facilitate proliferation of chondrocytes, production of sulfated glycosaminoglycans and type II collagen, as well as the formation of neocartilage with specific, reproducible 3-dimensional shapes and histological features that closely resemble cartilage (9, 10). Although sponges, foams, and matrices with defined porosities are useful for the fabrication of relatively large and highly porous 3-dimensional analogs of the extracellular matrix, their use is limited for the creation of a basal lamina, a thin membranous layer of connective tissue found in many organs and tissues.

The basal lamina performs several important functions in a variety of tissues. In the glomerulus of the kidney, the basal lamina separates endothelial cells from podocytes and acts as a selectively permeable barrier to plasma molecules (reviewed in ref 11). In the skin, the basal lamina functions as a barrier that separates cells (epidermal keratinocytes) from un-

¹ Correspondence: Shriners Hospital for Children, 51 Blossom St., Boston, MA 02114, USA. E-mail: jmorgan@sbi.org.

derlying connective tissue (dermis). Although it prevents fibroblasts in the dermis from contacting epidermal keratinocytes, it does not prevent the movement of immune cells in and out of the epidermis, nor does it prevent the innervation of the epidermis. During wound healing as well as during normal development, the basal lamina acts as a guide and template that helps control cell migration and differentiation (12). As with most tissues, the basal lamina in the skin is not a simple flat plane of connective tissue, rather it conforms to a series of ridges and invaginations known as rete ridges and papillary projections. In addition to effects on the biomechanical properties of the skin, the pattern and depths of these ridges are thought to have a role in the proliferation and differentiation of epidermal keratinocytes. The fabrication of a basal lamina with controlled dimensions would help elucidate the influence of topography on cell function and should have applications in tissue engineering of skin substitutes as well as other basal lamina-containing tissues.

In this study, we used a microfabrication approach to produce an analog of a basal lamina with precisely engineered topographic features. After designing a test pattern with features comparable in length scale to the topographic features of native basal lamina structures, a master chip was created by laser machining the geometric specifications into a polyimide chip. Using negative replicates of the chip, we produced thin, biocompatible membranes with topographic features that reproduced the dimensions of the master chip. The utility of the microfabricated membrane was demonstrated by laminating it to the surface of a collagen sponge to form a composite analog of the dermis. When epidermal keratinocytes were cultured on the surface of this composite, the cells formed a continuous, translucent, and hydrophobic epidermis with gross topographic features that conformed to the surface of the microfabricated membrane.

MATERIALS AND METHODS

Microfabrication of a master chip and negative replicates

The production of a microfabricated analog of a basal lamina began with the design of a test pattern. To test the range of sizes over which we could control the topography of these membranes, we designed a test pattern with a series of parallel channels (10 mm long) of various widths (40 to 200 μm) and depths (40 to 200 μm). A master chip was produced by laser machining (Potomac Photonics, Inc., Lanham, Md.) these specified channels into a polyimide chip (1.0 mm thick; Goodfellow Corp., Berwyn, Pa.). Briefly, rectangular images of an Excimer laser beam were focused onto the surface of a polyimide chip, then the laser energy was pulsed to ablate its surface. The image of the laser beam was repositioned and the process was repeated until channels with the specified

geometries were machined. To make negative replicates, a solution of liquid polydimethylsiloxane silicone elastomer (PDMS; Sylgard 184, Dow Corning Corp., Midland, Mich.) was poured over the master chip and polymerized by incubation at 65°C for 2 h. The PDMS overlay, which conformed to the fine features (e.g., channels) of the master chip, was carefully separated from the chip. The resulting negative replicates had surfaces of protruding ridges that were a replicate of the channels of the master chip.

Production of a basal lamina analog

Two types of materials were used with the negative replicates to make membranes: gelatin or a white coprecipitate containing type I collagen (5 mg/ml) and glycosaminoglycan (GAG, 0.18 mg/ml). A 1% (w/v) gelatin solution was prepared by stirring 1.0 g of gelatin (Sigma Chemical, St. Louis, Mo.) into 100 ml of a 0.05 M acetic acid solution that was warmed to 65°C until the gelatin was completely dissolved. The coprecipitate was prepared according to published protocols (6). Briefly, 3.6 g of lyophilized bovine collagen (Medicol F, Integra Medicus, West Chester, Pa.) was dispersed in 600 ml of a 0.05 M acetic acid solution by blending at 20,000 rpm for 90 min at 4°C in a refrigerated homogenizer. The coprecipitate was formed by adding 120 ml of a 0.11% w/v solution of shark cartilage chondroitin 6-sulfate (Sigma Chemical) to the blending collagen dispersion, then blending the collagen-GAG copolymer for an additional 90 min. The collagen-GAG dispersion was degassed under vacuum to remove trapped air, then stored at 4°C.

To create membranes, a small volume of either gelatin or collagen-GAG dispersion (220–330 $\mu\text{l}/\text{cm}^2$) was poured onto the PDMS-negative replicate, where it conformed to the surface. The dispersion was air-dried overnight at room temperature in a laminar flow hood and the resulting dried collagen membrane was gently peeled from the negative replicate. Finally, dried membranes were covalently cross-linked by thermal dehydration at 105°C in a vacuum of 100 mTorr for 24 h.

Production of a dermal analog

Composite dermal analogs were prepared by laminating a microfabricated membrane to the surface of a collagen sponge. The collagen sponge was produced by methods similar to those previously described by Yannas et al. (13) and Boyce et al. (14). Briefly, 10 ml of collagen-GAG dispersion was poured into an aluminum pan with a surface area of 38.5 cm^2 (Fisher Scientific, Springfield, N.J.), and a microfabricated membrane was gently floated on the surface of the dispersion. The dispersion was rapidly frozen at -80°C , placed on a shelf in a freeze dryer initially set at -45°C , then lyophilized overnight (Virtis Genesis, Virtis, Gardner, N.Y.) at a vacuum of 100 mTorr. After lyophilization, the composites were covalently cross-linked by thermal dehydration at 105°C in a vacuum of 100 mTorr for 24 h, rehydrated in a 0.05 M acetic acid solution for 24 h, cross-linked in a 0.25% glutaraldehyde solution for 24 h, then washed exhaustively with sterilized water, PBS, and keratinocyte seeding medium (described below).

Keratinocyte culture

Normal human keratinocytes derived from neonatal foreskins were cultured by the method of Rheinwald and Green (15). Keratinocytes were cocultivated with 3T3-J2 mouse fibroblasts (originally provided by H. Green, Harvard Medical School, Boston, Mass.) that had been pretreated with 15 $\mu\text{g}/\text{ml}$

mitomycin C (Boehringer Mannheim Co., Indianapolis, Ind.). Culture medium was changed every 3–4 days with a 3:1 mixture of Dulbecco's modified Eagle's medium (DMEM) (high glucose) (Life Technologies, Inc.-BRL, Gaithersburg, Md.) and Ham's F-12 medium (Life Technologies, Inc.-BRL) with 10% fetal bovine serum (FBS; JRH Bioscience, Lenexa, Kans.). Supplements were added as described previously (16). Cells were subcultured by first removing the feeder layer cells with a brief EDTA wash, 5 mM in phosphate-buffered saline (PBS), and then treating the keratinocytes with trypsin-EDTA.

Production of skin equivalents

Keratinocytes were seeded onto the dermal analogs using methods similar to those previously described (17) with media changes as described by Ponec et al. (18). Dermal analogs were placed into 35 mm tissue culture dishes, microfabricated membrane side up, and cells in keratinocyte seeding medium (described below) were seeded onto the surface (5×10^5 cells/cm²). After ~2 h, the cell-seeded dermal analogs were submerged in keratinocyte seeding medium for 24 h. Keratinocyte seeding medium was a 3:1 mixture of DMEM (high glucose) (Life Technologies, Inc.-BRL) and Ham's F-12 medium (Life Technologies, Inc.-BRL) supplemented with 1% FBS (JRH Bioscience), 10^{-10} M cholera toxin (*Vibrio Cholerae*, Type Inaba 569 B; Calbiochem, La Jolla, Calif.), 0.2 µg/ml hydrocortisone (Calbiochem), 5 µg/ml insulin (Novo Nordisk, Princeton, N.J.), 50 µg/ml ascorbic acid (Sigma Chemical), and 100 IU/ml and 100 µg/ml penicillin-streptomycin (Boehringer Mannheim Co.). After 24 h, keratinocyte seeding medium was removed and the skin equivalents were submerged for an additional 48 h in a keratinocyte priming medium. Keratinocyte priming medium was composed of keratinocyte seeding medium supplemented with 24 µM bovine serum albumin, 1.0 mM L-serine, 10 µM L-carnitine, and a mixture of fatty acids including 25 µM oleic acid, 15 µM linoleic acid, 7 µM arachidonic acid, and 25 µM palmitic acid, all from Sigma Chemical (19). After 48 h in priming medium, skin equivalents were placed on stainless steel screens, raised to the air-liquid interface, and cultured for 7 days with an air-liquid interface medium composed of serum-free keratinocyte priming medium supplemented with 1.0 ng/ml epidermal growth factor (Collaborative Biomedical Products, Bedford, Mass.).

Histological and quantitative morphometric analyses

For histological analysis, skin equivalents were fixed in a 3% glutaraldehyde/4% paraformaldehyde solution, dehydrated with increasing concentrations of ethanol, infiltrated first at -80°C and then at 4°C with glycolmethacrylate (JB-4, Polysciences, Inc., Warrington, Pa.), and finally embedded in glycolmethacrylate. Sections of skin equivalents, 5 µm in thickness, were collected by cutting samples in a plane perpendicular to the surface of the microfabricated membrane. Sections were mounted on glass slides with Tissue-Tack Adhesive (Polysciences, Inc.), stained with Gill's hematoxylin and ethanolic eosin solutions, then viewed with a Nikon Eclipse 800 microscope. The dimensions of the channels in a collagen membrane were measured in triplicate with a Nikon Diaphot 300 microscope coupled to MetaMorph Imaging Software (West Chester, Pa.). The thickness of the stratified epidermal layer in each channel and between channels was measured vertically from the lower surface of the basal layer to the outer edge of the granular layer. Conversely, invaginations of the epidermal layer in each channel were measured vertically the granular layer at the bottom of each channel up

to the plane that corresponded to the granular layers of the adjacent interchannel regions.

For scanning electron microscopy, skin equivalents were fixed in a 3% glutaraldehyde/4% paraformaldehyde solution, postfixed with a 1% osmium tetroxide solution, en bloc stained with a 2% uranyl acetate solution, dehydrated with increasing concentrations of ethanol, then critical point dried with liquid carbon dioxide under pressure. Samples were sputter coated with a thin layer of gold-palladium and viewed with an Amray 1000 scanning electron microscope.

The dimensions of the channels in the laser machined master chip were analyzed with a Zygo New View 200 Scanning White Light Interference Microscope (Zygo Corp., Middlefield, Conn.) fitted with a $20\times$ Mirau objective lens. The microscope produced 3-dimensional images of each channel and 2-dimensional surface profiles in planes perpendicular to the surface of the master chip. The shoulder-to-shoulder widths and maximum depths of each channel were measured with the caliper tools in the microscope software.

The dimensions of the channels on a PDMS-negative replicate were analyzed with a Nikon Diaphot 300 microscope coupled with MetaMorph Imaging Software. Sections of a negative replicate were collected by cutting samples in a plane perpendicular to the microfabricated surface with a razor blade. Sections were placed on glass slides, viewed with a low power objective lens, and digitally imaged with the microscope software. Shoulder-to-shoulder widths and maximum depths of each channel were measured in triplicate with the tools provided in the software package.

RESULTS

Channels of varied widths and depths can be laser machined into a single polyimide chip

To test the feasibility of producing a biocompatible membrane with complex topographic features similar in length scale to those found in naturally occurring basal lamina, we began by designing a test pattern. This test pattern consisted of five sets of channels with widths that ranged from 40 to 200 µm and depths that increased stepwise by 40 µm per set, from 40 to 200 µm (Fig. 1). Our strategy was to create a single master chip that could be used as a template to produce numerous negative replicates that could then be used to produce membranes with topographic features corresponding to the design in the master chip. The master chip was produced by laser machining our specified test pattern into the surface of a single polyimide chip (Fig. 1).

To test the fidelity with which laser machining satisfied the specifications of our design, we measured the dimensions of the channels in the master chip by Scanning White Light Interference (SWLI) microscopy. SWLI microscopy provided noncontact quantitative 2- and 3-dimensional topographic data with submicron resolution for each of the channels, although its ability to image vertical surfaces such as the side walls of some channels was limited. SWLI images of the master chip showed that the narrow channels (specified widths: 40 or 80 µm) had

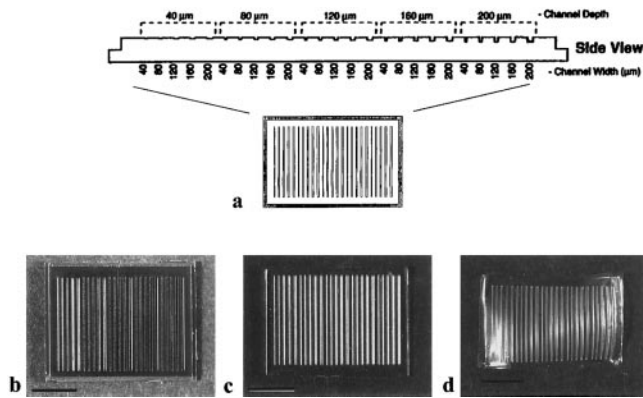


Figure 1. Design and microfabrication of a master chip, a negative replicate, and a microfabricated basal lamina. Diagram of a test pattern consisting of a series of parallel channels with varied widths and depths (*a*). Photographs show *b*) a master chip made by laser machining the specified channels into the surface of a polyimide chip, *c*) a negative replicate formed by curing polydimethylsiloxane (PDMS) on the surface of the master chip, and *d*) a microfabricated membrane produced by air-drying a small volume of gelatin or collagen-GAG coprecipitate on the surface of the negative replicate. The scale bars represent 5.0 mm.

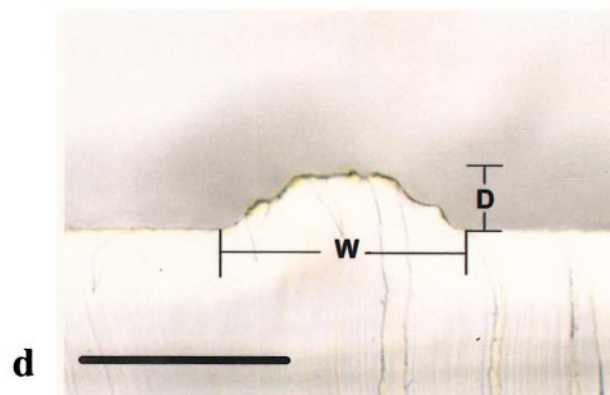
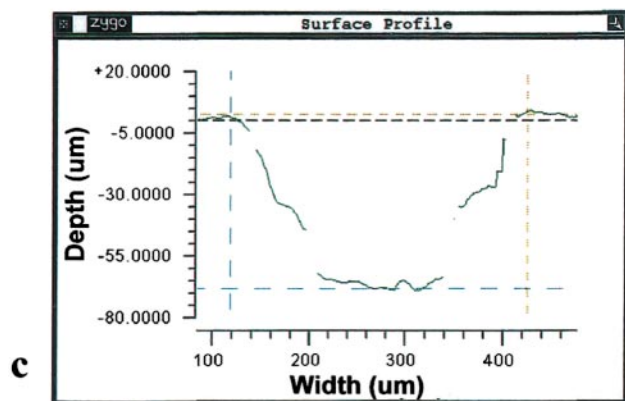
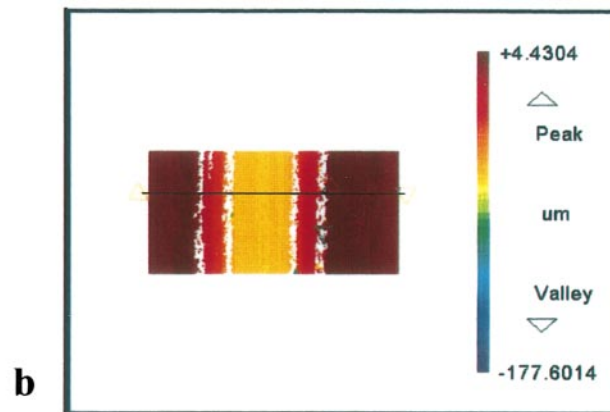
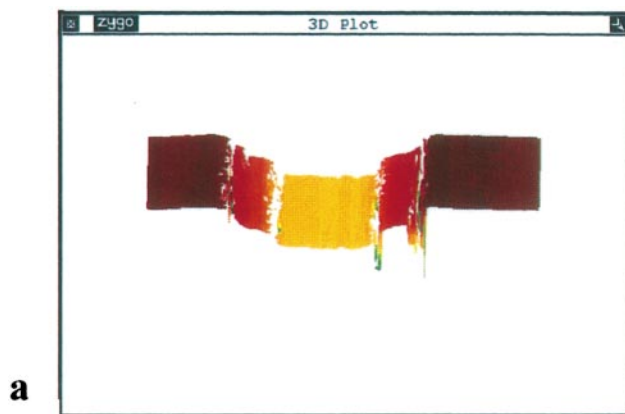
smooth side walls and flat bottom surfaces close to the original design. Conversely, the bottom surfaces of the wider channels (specified widths: 120, 160, or 200 μm) tapered to points or had irregular surfaces. In addition, the widest channels (specified width:

200 μm) had notched shoulders in the side walls (Fig. 2). Since the shapes of the channels were not rectangular, we simplified and standardized our quantitative analyses by measuring the maximum shoulder-to-shoulder width and maximum depth of each channel (Fig. 2). Although the widths in the master chip deviated from the original design, they covered a range of widths from 114 to 310 μm , with five distinct channel widths (Table 1). For example, channels whose width was specified to be 40 μm had an average maximum width of $117 \pm 3 \mu\text{m}$ for all depths specified.

The maximum channel depths, with some exceptions, were closer to the design specifications (Table 1) and covered a range of depths from 42 to 290 μm . For example, channels whose depth was specified to be 40 μm had an average maximum depth of $62 \pm 21 \mu\text{m}$ for all widths specified. Some depths, such as those channels whose width was specified to be 120 μm , were consistently deeper than specified.

PDMS faithfully replicates the polyimide chip

To make negative replicates of the master chip, we poured liquid PDMS over the polyimide chip and polymerized the PDMS by heat curing (Fig. 1). To determine whether PDMS had faithfully replicated the features of the master chip, we sectioned the



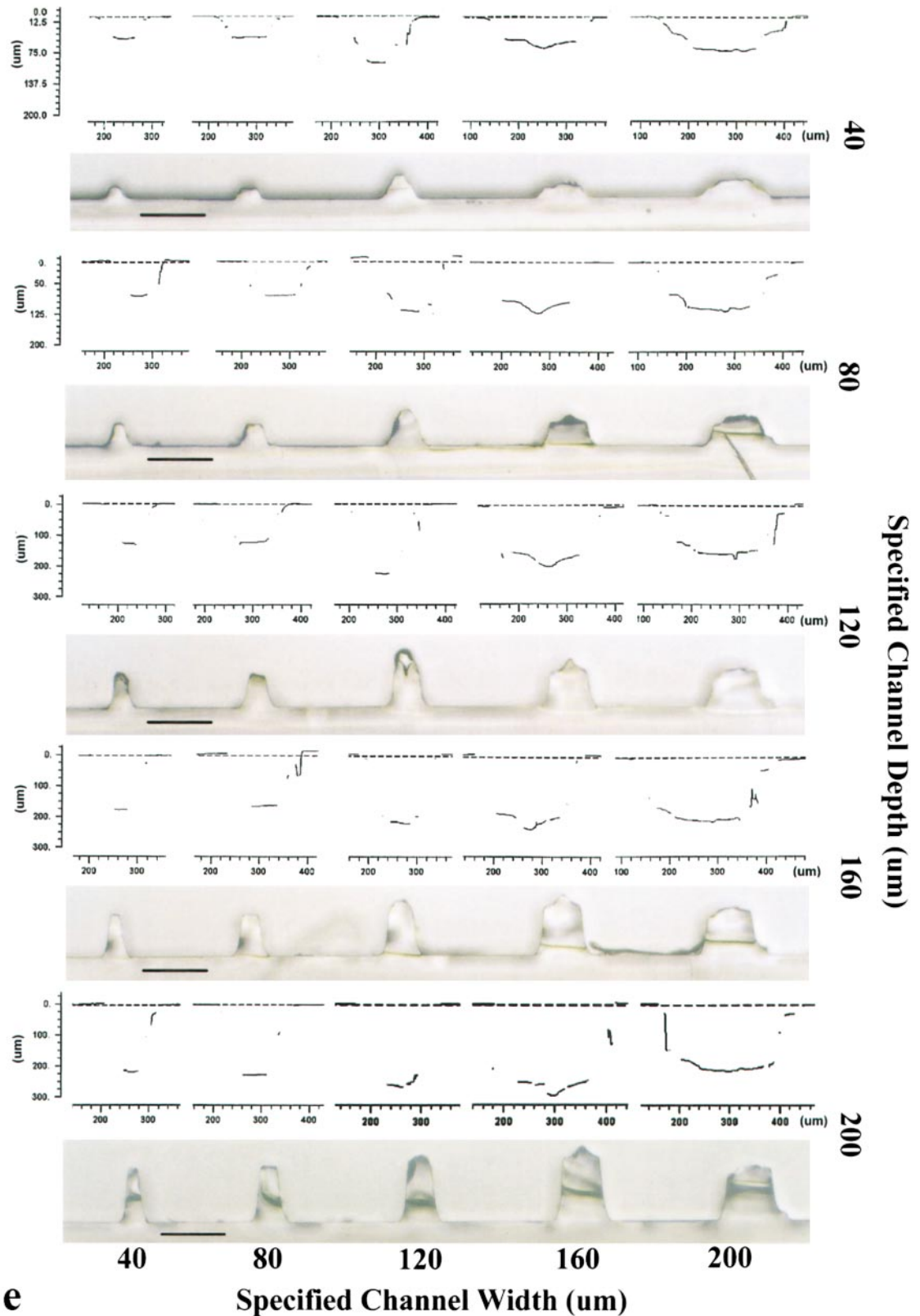


Figure 2. Morphometric analyses of the master chip and a negative replicate. *a*) 3-Dimensional plot of a typical channel in the master chip produced by a SWLI microscopy. *b*) Surface plot of a channel (top view), used to select a plane perpendicular to the surface of the master chip for morphometric analysis. *c*) 2-Dimensional surface profile in the selected plane, used to measure the width and depth of each channel. *d*) Sections cut perpendicular to the surface of a negative replicate, used to measure the width (*w*) and depth (*d*) of the protruding ridges. *e*) Composite figure comparing the dimensions of each protruding ridge of the negative replicate with the surface profile of the corresponding channel in the master chip. The scale bars represent 250 μm (*d*, *e*).

TABLE 1.

Channel width (μm)		
Test pattern (Specified)	Master chip (Actual)	Negative replicate (Actual)
40	117.6 ± 3.05	119.0 ± 6.67
80	153.2 ± 4.87	152.5 ± 9.48
120	179.0 ± 9.43	175.0 ± 7.02
160	238.6 ± 8.47	230.5 ± 8.05
200	300.2 ± 9.68	298.9 ± 9.90
Channel depth (μm)		
Test pattern (Specified)	Master chip (Actual)	Negative replicate (Actual)
40	62.4 ± 21.23	60.5 ± 18.56
80	109.2 ± 22.53	108.4 ± 22.77
120	166.8 ± 42.69	162.9 ± 36.53
160	202.4 ± 27.19	198.5 ± 28.92
200	242.6 ± 34.2	241.5 ± 32.58

PDMS and measured the maximum shoulder-to-shoulder width and maximum depth of each of the protruding PDMS ridges (Fig. 2). When compared to the values from the master chip, there was no significant difference over the entire range of widths and depths (Table 1). Thus, PDMS had faithfully replicated the polyimide chip and had even replicated many of the small (micron) irregular features found in the bottom of some of the channels.

Thin membranes with complex topographies can be laminated to a porous collagen sponge

To determine the dimensions over which we could microfabricate topographic features in a thin, biocompatible membrane, we poured a small volume of gelatin or collagen-GAG coprecipitate onto the negative replicates. The solutions were air-dried; membranes with features similar to the master chip could be gently peeled off the negative replicates (Fig. 1).

To form a composite dermal analog, these membranes were floated on the surface of a small volume of collagen-GAG coprecipitate, which was subsequently frozen and lyophilized to form a collagen-GAG sponge (Fig. 3). Scanning electron micrographs of a cross section of these composites (Fig. 3) showed that the surface of a highly porous collagen/GAG sponge had been laminated with a thin membrane containing a series of channels.

To determine whether the membranes had reproduced the surface of the negative replicate, we rehydrated a composite and analyzed the dimensions of the channels in the membrane. After rehydration, we observed that the thin membrane became supple and flexible. The dermal equivalent was subsequently fixed, embedded in glycolmethacrylate, and sections were cut perpendicular to the surface. Depending on the volume of collagen/GAG

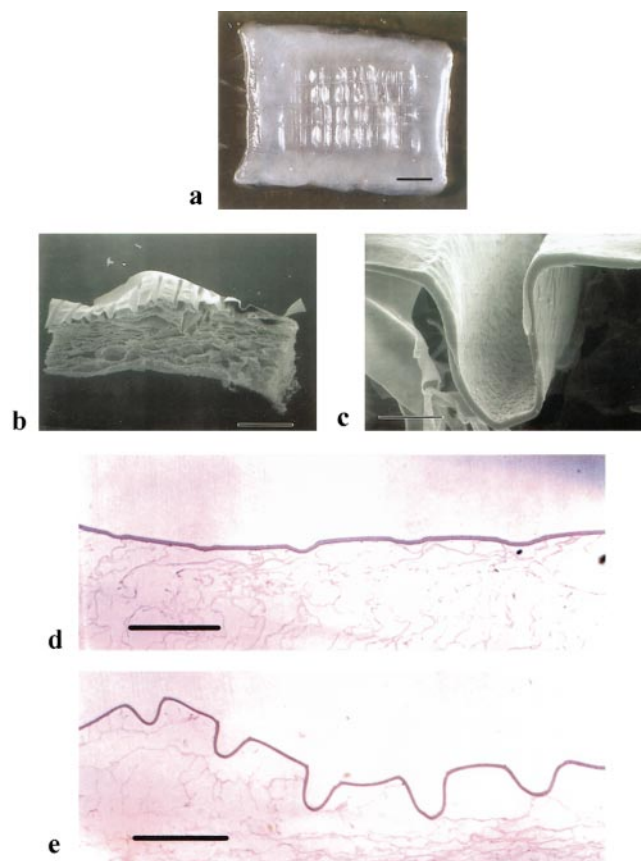


Figure 3. Composite dermal equivalent with a microfabricated membrane. *a*) Photograph of a rehydrated dermal analog, produced by laminating a microfabricated membrane to the surface of a collagen-GAG sponge. Scanning electron micrographs of a dermal analog (*b*) and higher magnification of a microfabricated channel (*c*). Hematoxylin and eosin stained sections cut perpendicular to the surface of the skin equivalent show a microfabricated membrane, with the shallowest (*d*) or deepest set of channels (*e*). Scale bars represent 5.0 mm (*a*), 1.0 mm (*b*), 50 μm (*c*), or 500 μm (*d*, *e*).

or gelatin used, the microfabricated membranes ranged in thickness from 21.7 ± 4.1 to 30.5 ± 7.1 μm , with 25 channels that were supported by a porous collagen-GAG sponge. Distinct widths and depths were produced in the membrane (Fig. 3) as well as many of the small irregular surface features that were observed in the negative replicate (Figs. 2 and 3). In contrast to the polyimide chip and the PDMS, the flexibility of these membranes, particularly the deepest channels, precluded the accurate measurements of the width and depth of the channels. Nevertheless, we estimated the fidelity of these membranes by measuring the perimeter of each channel and comparing it to the PDMS negative replicate. There was excellent correlation between the perimeters of the membrane and its corresponding PDMS replicate (Fig. 4).

An epidermis with complex topography can be formed on the surface of a microfabricated membrane

To investigate the response of cells to the topographic features of these membranes, cultured keratinocytes were seeded on the surface of the composite dermal analogs. The resulting skin equivalents were cultured at the air-liquid interface to induce differentiation and cornification of the epidermal layer. After 10 days, a continuous, translucent, and hydrophobic epidermis that conformed to the microfabricated surface of the skin equivalent was evident by gross inspection. Histological analyses showed that the surface of the skin substitute contained a series of channels of varied depths and

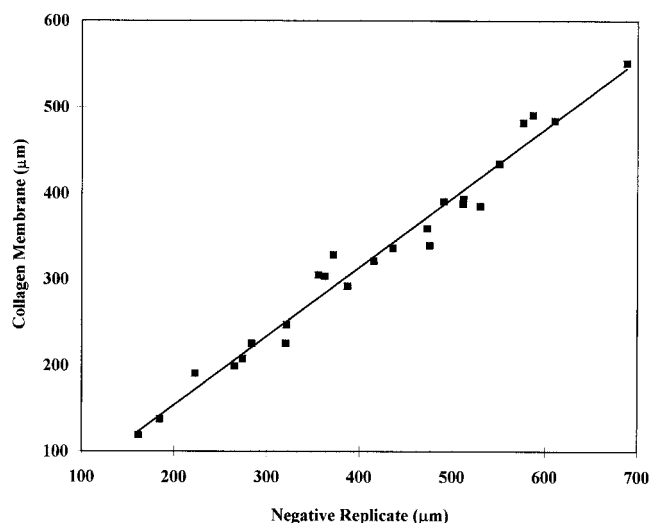


Figure 4. Morphometric traces of channel perimeters. The perimeter of each channel of the membrane was compared to the perimeter of its corresponding PDMS negative replicate. Negative replicates were measured in duplicates and collagen membranes were measured in triplicates. For linear regression line, $r^2=0.974$.

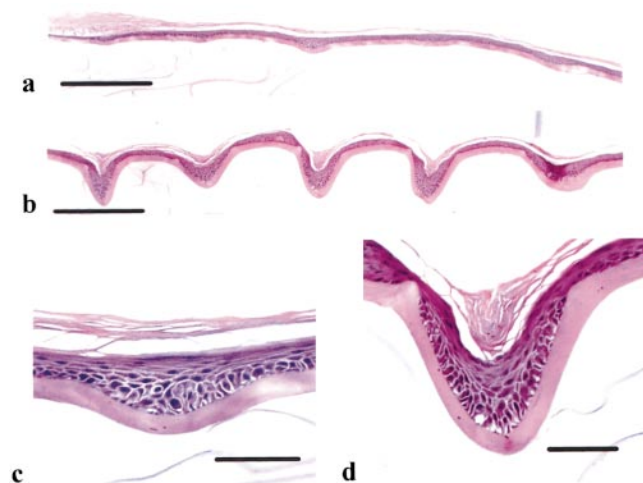


Figure 5. Skin equivalent with a microfabricated analog of the basal lamina. Keratinocytes were seeded on the surface of a composite dermal analog and grown at the air/liquid interface. Low magnification of a skin equivalent with the shallowest (a) or deepest set of channels (b). High magnification micrographs show differentiated and stratified keratinocytes in individual channels of a microfabricated membrane (c, d). Scale bars represent 500 μm (a, b) or 100 μm (c, d).

widths, as well as spaces between channels, covered with a stratified epidermis (Fig. 5).

Stratification of the deeper channels was enhanced compared to the shallower channels or the flat interchannel regions. To quantitate this response, we measured the thickness of the epidermal layer in each channel. Epidermal thickness of the flat interchannel regions was 37.1 μm and thickness increased as the depth of each channel was increased (Fig. 6). The best fit for this relationship was for those channels whose widths were between 250 and 350 μm .

It was also apparent that the channels induced the formation of invaginations of the epidermal surface. To determine the influence of channel geometry on these gross skin surface features, we also measured the distance of the epidermal invagination for each channel. Infolds of the epidermis occurred when the depth of the channels were greater than ~ 25 μm , and these invaginations increased in distance as channel depth increased (Fig. 6). The best fit was also for those channels whose widths were in the range of 250 to 350 μm .

DISCUSSION

The goal of this study was to investigate the feasibility of using microfabrication techniques to produce a membrane with complex topographic features similar to those of a basal lamina. A test pattern was produced by laser machining a polyimide master chip, and precise negative replicates were made by

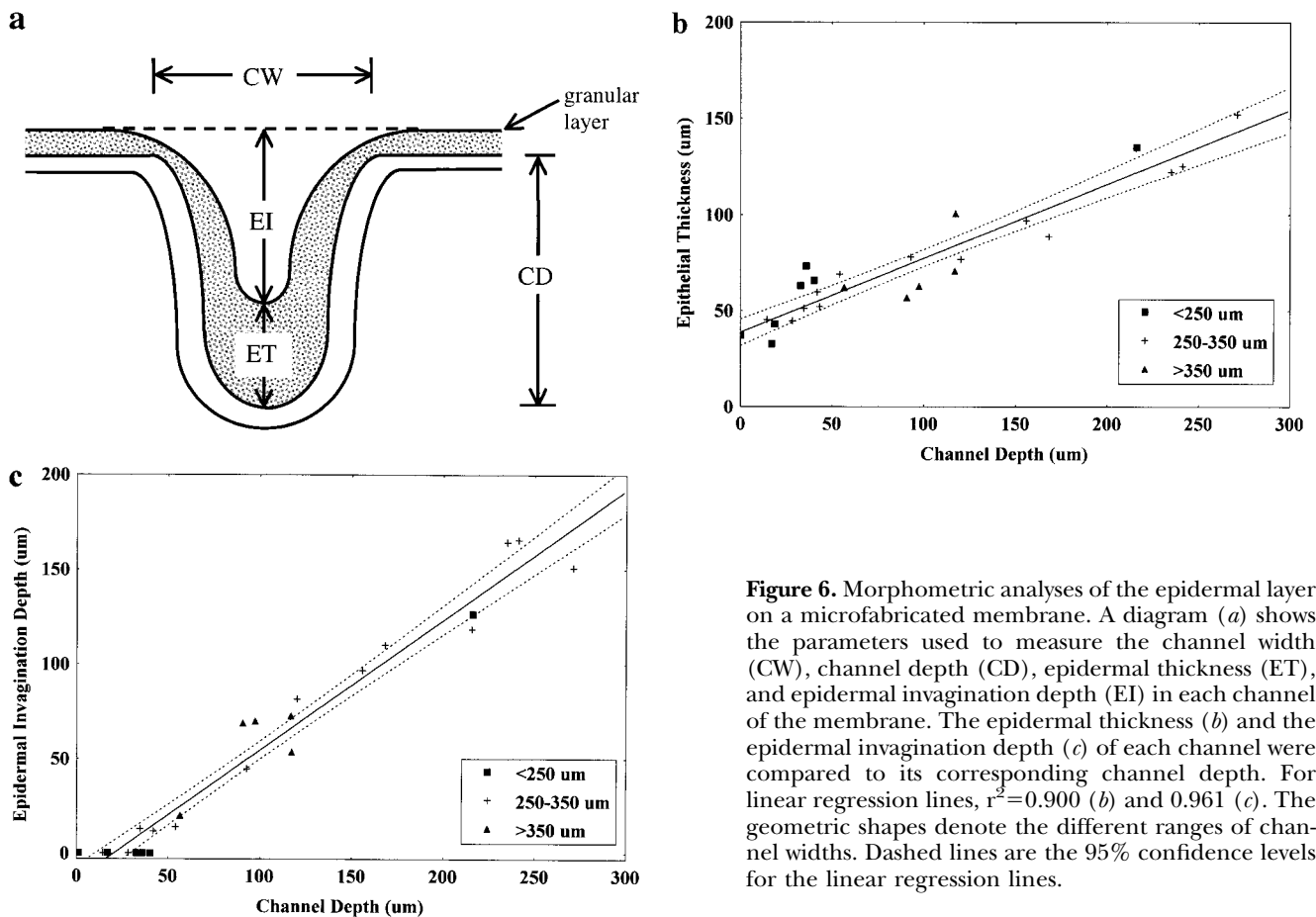


Figure 6. Morphometric analyses of the epidermal layer on a microfabricated membrane. A diagram (a) shows the parameters used to measure the channel width (CW), channel depth (CD), epidermal thickness (ET), and epidermal invagination depth (EI) in each channel of the membrane. The epidermal thickness (b) and the epidermal invagination depth (c) of each channel were compared to its corresponding channel depth. For linear regression lines, $r^2=0.900$ (b) and 0.961 (c). The geometric shapes denote the different ranges of channel widths. Dashed lines are the 95% confidence levels for the linear regression lines.

polymerizing liquid silicone elastomer on its surface. Using the negative replicates as templates, we created thin membranes with complex topographies that reproduced the key features of the master chip. These microfabricated membranes were laminated to the surface of a collagen sponge and seeded with keratinocytes to create a composite skin equivalent. The keratinocytes formed a translucent, hydrophobic epidermis with gross topographic features that correlated with the microfabricated surface of the membrane. Histological analyses showed that the epidermal layer was composed of differentiated and stratified keratinocytes that conformed to the surface of the skin equivalent, forming rete ridge-like structures comparable in dimension to those observed in native skin. Moreover, stratification was enhanced in the deeper channels.

Native basal laminae exhibit a range of thickness (50–90 nm in skin to 240–340 nm in kidney glomerulus) and contain a variety of collagenous and non-collagenous extracellular matrix molecules, as well as sulfated proteoglycans. Although the exact composition varies between tissues, all basement membrane structures are believed to contain type IV collagen, laminin, fibronectin, and heparin sulfate proteoglycan (reviewed in ref 20). The function of basal laminae can also vary, but generally laminae act as

adhesive membranes that separate cell types or anchor epithelial cell layers to mesenchymal tissue. In addition to maintaining complex spatial organization of tissues (skin, intestinal mucosa, mammary ducts, and salivary glands), they can also act as a selective barrier to cells and macromolecules.

Our study demonstrates for the first time that microfabrication approaches can be used to produce analogs of the basal lamina and that these first analogs exhibit some, but not all, properties of native basal laminae. Principally, these analogs served as membranes that supported the attachment and growth of keratinocytes in complex topographies and prevented keratinocytes from passing through, while allowing for the diffusion of nutrients. Compared to a native basal lamina (50–340 nm), these analogs were relatively thick, in the range of 21 μm ; however, future efforts to optimize the production of thinner membranes should be able to reduce this thickness considerably.

Another difference from a native basal lamina is composition. Although the analogs in this study were produced with type I collagen or gelatin, our preliminary data shows that similar membranes can be produced with material containing type IV collagen, laminin, fibronectin, and proteoglycans. Thus, microfabricated analogs with different macromolecular

compositions should be useful for investigating the role of various macromolecules in basal lamina structure/function and how these structure/functions are influenced by topography.

The microfabrication technology we chose for this study was based on laser machining a polyimide chip. This approach, although extremely useful for generating a single test pattern with a wide range of widths and depths, has some drawbacks. Our measurements of the chip and the negative replicates show that the fidelity with which the laser was able to machine the specified design was not as accurate as might be desired for some applications. Other microfabrication technologies, such as photolithography, can be used to generate patterns that more accurately reflect the intended design. Moreover, this technology can be used to produce topographies far more complex than the parallel channels in our master chip. For example, photolithography could easily be used to create a pattern of hexagonally packed arrays of pegs that mimic the dermal papillae in native skin.

Stratification of the epidermis was significantly enhanced in the deep channels, as is the case for rete ridges of normal skin. This finding suggests that the topographical microenvironment influences keratinocyte differentiation/proliferation by affecting the spatial arrangement of cell-matrix contacts and/or cell-cell contacts. Note that in human palmar epidermis, the highest percentage (80%) of the proliferating basal and suprabasal cells is in the deeper rete ridges (21). It has also been shown that expression of $\alpha_2\beta_1$ integrin, a marker of epidermal stem cells, also varies with topography. High expression is found in patches of basal cells located on the tips of the dermal papillae (foreskin, scalp) or at the bottom of the deep rete ridges (palm) (22, 23). A microfabricated membrane may be a useful tool to examine the relationship between the dimensions of topographic features and the proliferation and differentiation of basal keratinocytes in the epidermis.

Microfabricated membranes may be useful for investigating the critical topographical features of skin that contribute to its mechanical stability. In areas of the skin exposed to excessive friction (plantar and palmar surfaces), the dermal papillae and epidermal ridges are longer and more numerous, suggesting that the enhancement of the interface between the epidermis and dermis helps provide additional mechanical stability (24). By testing the properties of skin equivalents that have rete ridges and dermal papillae of various geometries, it should be possible to establish a direct and quantitative link between topography and mechanical properties. Moreover, these studies can be extended to the molecular level by examining the distribution and numbers of known adhesive proteins such as integrins and hemidesmosomes (22, 25).

Previous studies have shown that tissue-engineered skin equivalents also have clinical application for the treatment of patients suffering from severe burns and chronic ulcers (reviewed in ref 26, 27). Boyce et al. produced a composite skin substitute by laminating the surface of a flat collagen sponge originally developed by Yannas et al. (13, 28). Fibroblasts were seeded into the porous collagen sponge and a flat epidermal layer was cultured on the laminated surface (14, 29). In clinical studies, these composite skin substitutes have had some success for the treatment of full-thickness burns (2). Another skin equivalent has been produced by culturing a flat epidermal layer on the surface of a fibroblast populated collagen gel (30). These skin equivalents have recently been approved for the treatment of venous leg ulcers (4). Recently, novel skin equivalents with capillary-like networks have also been produced (31).

Microfabricated membranes may be useful for improving the performance of these skin substitutes. Each of these skin equivalents has a flat interface between the epidermis and the dermal component. A microfabricated membrane that created a complex interdigitating interface between these two layers might be expected to improve the resistance of these skin substitutes to failure due to shear forces. Such a complex interface might also facilitate improved mass transport of nutrients and growth factors to the epidermis and aid in graft take. Moreover, since microfabrication can be used to create complex patterns, it should be possible to mimic the fine lines and pore structures of native skin to create a more 'natural' and perhaps cosmetically acceptable skin substitute.

Since basal lamina are an integral part of many other tissues besides skin, microfabricated membranes may have other applications in tissue engineering and developmental biology. For example, it may be possible to enhance mass transport in tissue-engineered small intestine by using a microfabricated membrane that mimics the topography of the intestinal mucosa. During development, it is well known that basal laminae perform critical roles in embryologic tissue compartmentalization and organized cellular migration leading to morphogenesis and organogenesis (reviewed in ref 20, 32). With the recent isolation of embryonic stem cell lines derived from human blastocysts (33), microfabricated analogs of the basal lamina may be useful for exploring the roles of cell and matrix interactions on tissue morphogenesis and mammalian development. **[F]**

The authors wish to thank the Core Morphology Facility at the Shriners Burns Hospital, the Microfabrication Facility in the Center for Engineering in Medicine at Massachusetts General Hospital, and Janet Cuy for assistance with the morphometric analyses. This work was supported in part by grants from the Shriners Hospital for Children and the National Institutes of Health (R29 AR42012-01A1) (J.R.M.).

REFERENCES

- Langer, R., and Vacanti, J. P. (1993) Tissue engineering. *Science* **260**, 920–926
- Boyce, S. T., Goresky, M. J., Greenhalgh, D. G., Kagan, R. J., Rieman, M. T., and Warden, G. D. (1995) Comparative assessment of cultured skin substitutes and native skin autograft for treatment of full-thickness burns. *Ann. Surg.* **222**, 743–752
- Stern, R., McPherson, M., and Longaker, M. T. (1990) Histologic study of artificial skin used in the treatment of full-thickness thermal injury. *J. Burn Care Rehabil.* **11**, 7–13
- Falanga, V., Margolis, D., Alvarez, O., Auletta, M., Maggiasomo, F., Altman, M., Jensen, J., Sabolinski, M., and Jardin-Young, J. (1998) Rapid healing of venous ulcers and lack of clinical rejection with an allogeneic cultured human skin equivalent. *Arch. Dermatol.* **134**, 293–300
- Brittberg, M., Lindahl, A., Nilsson, A., Ohlsson, C., Isaksson, O., and Peterson, L. (1994) Treatment of deep cartilage defects in the knee with autologous chondrocyte transplantation. *N. Engl. J. Med.* **331**, 889–895
- Chamberlain, L. J., and Yannas, I. V. (1998) Preparation of collagen-glycosaminoglycan copolymers for tissue regeneration. In *Tissue Engineering Methods and Protocols* (Morgan, J. R., and Yarmush, M. L., eds) pp. 3–17, Humana Press, Totowa, N.J.
- Yannas, I. V., Lee, E., Orgill, D. P., Skrabut, E. M., and Murphy, G. F. (1989) Synthesis and characterization of a model extracellular matrix that induces partial regeneration of adult mammalian skin. *Proc. Natl. Acad. Sci. USA* **86**, 933–937
- Wake, M. C., Patrick, C. W., Jr., and Mikos, A. G. (1994) Pore morphology effects on the fibrovascular tissue growth in porous polymer substrates. *Cell Transplant.* **3**, 339–343
- Freed, L. E., Marquis, J. C., Nohria, A., Emmanuel, J., Mikos, A. G., and Langer, R. (1993) Neocartilage formation in vitro and in vivo using cells cultured on synthetic biodegradable polymers. *J. Biomed. Mat. Res.* **27**, 11–23
- Freed, L. E., and Vunjak-Novakovic, G. (1995) Tissue engineering of cartilage. In *The Biomedical Engineering Handbook* (Bronzino, J. D., ed) pp. 1788–1806, CRC Press, Boca Raton, Florida
- Farquhar, M. G. (1991) The glomerular basement membrane - A selective macromolecular filter. In *Cell Biology of Extracellular Matrix* (Hay, E. D., ed) pp. 365, Plenum Press, New York, N.Y.
- Vracko, R. (1974) Basal lamina scaffold-anatomy and significance for maintenance of orderly tissue structure. *Am. J. Pathol.* **77**, 313–346
- Yannas, I. V., Burke, J. F., Gordon, P. L., Huang, C., and Rubenstein, R. H. (1980) Design of an artificial skin. II. Control of chemical composition. *J. Biomed. Mater. Res.* **14**, 107–131
- Boyce, S. T., Christianson, D. J., and Hansbrough, J. F. (1988) Structure of a collagen-GAG dermal skin substitute optimized for cultured human epidermal keratinocytes. *J. Biomed. Mater. Res.* **22**, 939–957
- Rheinwald, J. G., and Green, H. (1975) Formation of a keratinizing epithelium in culture by a cloned cell line derived from a teratoma. *Cell* **6**, 317–330
- Eming, S. A., Lee, J., Snow, R. G., Tompkins, R. G., Yarmush, M. L., and Morgan, J. R. (1995) Genetically modified human epidermis overexpressing PDGF-A directs the development of a cellular and vascular connective tissue stroma when transplanted to athymic mice: Implications for the use of genetically modified keratinocytes to modulate dermal regeneration. *J. Invest. Dermatol.* **105**, 756–763
- Medalie, D. A., Eming, S. A., Collins, M. E., Tompkins, R. G., Yarmush, M. L., and Morgan, J. R. (1997) Differences in dermal analogs influence subsequent pigmentation, epidermal differentiation, basement membrane, and rete ridge formation of transplanted composite skin grafts. *Transplantation* **64**, 454–465
- Ponec, M., Weerheim, A., Kempenaar, J., Mulder, A., Gooris, G. S., Bouwstra, J., and Mammaas, A. M. (1997) The formation of competent barrier lipids in reconstructed human epidermis requires the presence of vitamin C. *J. Invest. Dermatol.* **109**, 348–355
- Boyce, S. T., and Williams, M. L. (1993) Lipid supplemented medium induces lamellar bodies and precursors of barrier lipids in cultured analogues of human skin. *J. Invest. Dermatol.* **101**, 180–184
- Burgeson, R. E. (1987) Basement membranes. In *Dermatology in General Medicine* (Fitzpatrick, T. B., Eisen, A. Z., Wolff, K., Freedberg, I. M., and Austen, K. F., eds) pp. 288–303, McGraw-Hill, New York, N.Y.
- Lavker, R. M., and Sun, T.-T. (1983) Epidermal stem cells. *J. Invest. Dermatol.* **81**, 121s–127s
- Carter, W. G., Symington, B. E., and Kaur, P. (1992) Cell adhesion and the basement membrane in early epidermal morphogenesis. In *Epithelial Organization and Development* (Fleming, T. P., ed) pp. 299–327, Chapman and Hall, London
- Jones, P. H., Harper, S., and Watt, F. M. (1995) Stem cell patterning and fate in human epidermis. *Cell* **80**, 83–93
- Odland, G. F. (1950) The morphology of the attachment between the dermis and the epidermis. *Anat. Record* **108**, 399–413
- Burgeson, R. E. (1993) Dermal-epidermal adhesion in skin. In *Molecular and Cellular Aspects of Basement Membranes* (Rohrbach, D. H., and Timpl, R., eds) pp. 49–66, Academic Press, New York
- Morgan, J. R., and Yarmush, M. L. (1997) Bioengineered skin substitutes. *Sci. Med.* **4**, 6–15
- Teumer, J., Hardin-Young, J., and Parenteau, N. L. (1998) Tissue engineered skin. In *Frontiers in Tissue Engineering* (Patrick, C. W., Jr., Mikos, A. G., and McIntire, L. V., eds) pp. 664–677, Pergamon, New York
- Yannas, I. V., Burke, J. F., Orgill, D. P., and Skrabut, E. M. (1982) Wound tissue can utilize a polymeric template to synthesize a functional extension of skin. *Science* **215**, 174–176
- Boyce, S. T., and Hansbrough, J. F. (1988) Biologic attachment, growth and differentiation of cultured human epidermal keratinocytes on a graftable collagen and chondroitin-6-sulfate substrate. *Surgery* **103**, 421–430
- Bell, E., Ehrlich, H. P., Buttle, D. J., and Nakatsuji, T. (1981) Living tissue formed *in vitro* and accepted as skin-equivalent tissue of full thickness. *Science* **211**, 1052–1054
- Black, A. F., Berthod, F., L'Heureux, N., Germain, L., and Auger, F. A. (1998) *In vitro* reconstruction of a human capillary-like network in a tissue-engineered skin equivalent. *FASEB J.* **12**, 1331–1340
- Eklblom, P. (1993) Basement membranes in development. In *Molecular and Cellular Aspects of Basement Membranes* (Rohrbach, D. H., and Timpl, R., eds) pp. 359–383, Academic Press, New York
- Thomson, J. A., Itskovitz-Eldor, J., Shapiro, S. S., Waknitz, M. A., Swiegiel, J. J., Marshall, V. S., and Jones, J. M. (1998) Embryonic stem cell lines derived from human blastocysts. *Science* **282**, 1145–1147

Received for publication February 19, 1999.
Accepted for publication September 23, 1999.